Accuracy and Directional Sensitivity of the Single-Wire Technique

T. W. Jackson*
University of Maryland, College Park, Maryland
and
D. G. Lilley†
Oklahoma State University, Stillwater, Oklahoma

Multiorientation of a single normal hot wire is a novel way to measure the three time-mean velocities, three turbulent normal stresses, and three turbulent shear stresses. The present study focuses on the accuracy and directional sensitivity of the technique with respect to mean flow velocity orientation to the probe. Both nonswirling and swirling free jets are considered, using five probe configurations at each of five locations in the flowfield. Variation of input parameters and their effect on the output data has shown that the least accurate output quantities are the shear stresses, in particular the $x\theta$ component. The directional sensitivity analysis has shown that the technique adequately measures the properties of a flowfield independent of the dominant flow direction except when the flow is predominately in the direction of the probe holder. Results demonstrate relative insensitivity, indicating that the method is a useful cost-effective tool for turbulent flows of unknown dominant flow direction.

Nomenclature

A,B,C	= calibration constants
D	= test section diameter
d	= inlet nozzle diameter
E	= hot-wire voltage
G	= pitch factor
K	= yaw factor
$v=(u,v,w)$	= time-mean velocity (in x,r,θ directions) in facility coordinates
x,r,θ	= axial, radial, azimuthal cylindrical polar coordinates
Z	= effective cooling velocity acting on a wire
$\gamma_{Z_iZ_j}$	= correlation coefficient (estimated) between cooling velocities of adjacent wire orientations
ϕ	= swirl vane angle with respect to facility axis

Subscripts

0	= value at inlet to flowfield
rms	= root mean squared quantity

Superscripts

$\bar{(\ )}$	= time-mean average
$(\ )'$	= fluctuating quantity
$\tilde{(\ )}$	= relative to probe coordinates

I. Introduction

AT Oklahoma State University, Janjua[1] studied the six-orientation hot-wire probe technique, developed a suitable data reduction computer code, and presented results of its application in nonswirling free and confined jet flows. Jackson[2] extended the technique to investigate nonswirling and swirling nonreacting turbulent confined flows in an axisymmetric test section with expansion ratio $D/d=2$, which may be equipped with a strong contraction nozzle of area ratio 4 further downstream at $x/D=2$. The flowfield contains corner and central recirculation zones typical of gas turbine and ramjet combustion chambers. Swirl may be imparted to the incoming flow by means of a variable-angle vane swirler. The technique and its application to nonswirling and weakly swirling confined flows is described at length in Refs. 3 and 4. A recent paper[5] presents measurements for a *full* range of swirl strengths in the confined jet facility. This extended the data base given earlier[3] to higher inlet vane swirl angles, more axial measurement stations, and downstream nozzle effects. The data are being used to aid in the evolution of turbulence models for these complex flow situations.

The method is based upon earlier studies on multiorientation of a single normal hot wire. Dvorak and Syred[6] presented time-mean and turbulence property measurements in a complex flowfield with 45 deg between three successive orientations of the wire. A crossed-wire probe was additionally used to measure correlation coefficients. Measurements in swirling recirculating flows at the exit from a swirl generator were obtained with similar techniques, using up to six separate point measurements, by Syred et al.[7] Later, King[8] developed the six-orientation single normal hot-wire technique and applied it to vortex flows. There is some work on the use of a multiorientation single slant wire in turbulent flows, but its use in swirling flows is not yet established. For example, Arterberry[9] discusses the application of a 45 deg slanting wire suitable for weakly swirling flows. The present authors have restricted themselves to the normal wire configuration.

The aim of the present paper is to address questions about accuracy and directional sensitivity of the six-orientation, single normal hot-wire technique. An uncertainty analysis is performed on the data reduction procedure by changing individually strategic input parameters and noting their effect on deduced properties of the flow. A directional sensitivity analysis is presented that assesses the relative values of deduced flow properties (in facility coordinates) to local time-mean velocity orientation relative to the probe.

Essential features of the six-orientation, single hot-wire measurement technique are described briefly in Sec. II. The

Received Nov. 23, 1983; presented as Paper 84-0367 at the AIAA 22nd Aerospace Sciences Meeting, Reno, NV, Jan. 9-12, 1984; revision received May 1, 1985. This paper is declared a work of the U.S. Government and therefore is in the public domain.

*Assistant Professor, Department of Mechanical Engineering. Member AIAA.

†Professor, School of Mechanical and Aerospace Engineering. Associate Fellow AIAA.

directional sensitivity study is discussed in Sec. III and the mathematical coordinate transformations for velocity vectors and normal and shear stresses in Sec. IV. Results are presented and discussed in Sec. V and conclusions drawn in Sec. VI.

II. Measurement Technique

One of the most widely used instruments to obtain turbulence quantities is the hot-wire anemometer, the most common of which is the single hot wire. When used on a two-dimensional flow with a predominate flow direction, a single hot wire positioned normal to the main flow can be used to measure the streamwise components of the time-mean velocity and the rms velocity fluctuation in a standard manner.[9]

The anemometer used for the present study is DISA type 55M01, CTA standard bridge. A normal hot-wire probe, DISA type 55P01, is used in the experiments. This probe has two prongs set approximately 3 mm apart that support a 5 μm diameter wire, which is gold plated near the prongs to reduce end effects and strengthen the wire. The mean voltage is measured with a Hickok Digital Systems model DP100 integrating voltmeter and the rms voltage fluctuation is measured using a Hewlett Packard model 400 HR, ac voltmeter.

In a complex swirling flowfield, the dominant flow direction is unknown and the standard single-orientation single hot-wire method fails to supply sufficient information. The six-orientation method calls for a normal hot wire to be oriented through six different positions, each orientation separated by 30 deg from the adjacent one. Orientation 1 is normal to the facility centerline, orientation 2 is rotated 30 deg from this, etc. Mean and rms voltages are measured at each orientation. The data reduction is performed using assumptions that the turbulence follows a normal probability distribution having mean voltage as the mean and the squared value of the rms voltage as the variance. It is then possible to obtain the three time-mean velocity components, the three normal Reynolds stresses, and the three shear Reynolds stresses in the manner described here.

The six-orientation hot-wire technique requires a single straight hot wire to be calibrated for three different flow directions in order to determine the directional sensitivity of the probe. In the following relationships, tildes signify components of the instantaneous velocity vector in coordinates on the probe. Figure 1 shows how the $\tilde{u}$, $\tilde{v}$, and $\tilde{w}$ velocities in probe coordinate x, y, and z, respectively, are oriented with respect to the probe. In the usual radial traverse, the probe holder is aligned radially (as in case 1 of the five possible configurations subsequently studied). Then probe and facility coordinates coalesce and

$$[\tilde{u},\tilde{v},\tilde{w}]^T = [u,v,w]^T$$

$$[x,y,z]^T = [x,r,\theta]^T$$

Figure 1 also illustrates how rotating the probe holder sequentially yields the six orientations of the normal wire with respect to the facility main flow direction. The first orientation is with the wire perpendicular to the facility centerline (regardless of radial location), the second orientation is achieved by rotating the probe holder 30 deg about its axis, etc.

Each of the three calibration curves is obtained with zero velocity in the other two directions. The calibration curves demonstrate that the hot wire is most efficiently cooled when the flow is in the direction of the $\tilde{u}$ component (which is normal to both the wire and the supports). The wire is most inefficiently cooled when the flow is in the direction of the $\tilde{w}$ component (which is parallel to the wire). Each of the calibration curves follows a second order, least-square fit of the form

$$E_i^2 = A_i + B_i\tilde{u}_i^{1/2} + C_i\tilde{u}_i \qquad (1)$$

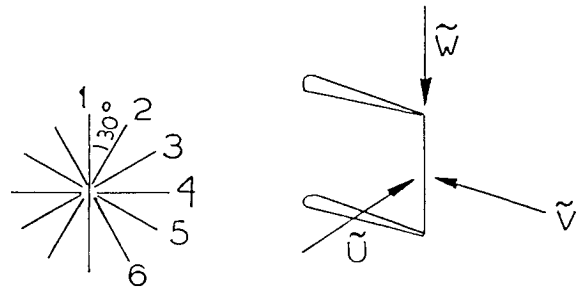

Fig. 1 Six orientations and probe coordinates.

which is an extension of the familiar King's law. In this equation, A_i, B_i, and C_i are calibration constants and $\tilde{u}_i$ can take on a value of $\tilde{u}$, $\tilde{v}$, and $\tilde{w}$ for the three calibration curves, respectively. This form of the cooling equation does not suffer from the problems of nonlinearity of response over a wide range of velocities, a problem encountered typically with the conventional King's law. This expression has been found[6] to give an excellent fit to calibration data over a velocity range of 1-60 m/s. It is expected that in a steady turbulent flowfield when using the six-orientation technique that vortex shedding will occur from the hot-wire prongs. This phenomenon is also expected in the calibration, especially in the $\tilde{w}$ direction. However, this vortex shedding is time dependent with short periodicity. In the turbulent flowfield, these effects are not time averaged out to zero, but are considered to be higher-order effects, which are very small and can essentially be considered negligible.

When the wire is placed in a three-dimensional flowfield, the effective cooling velocity experienced by the hot wire is

$$Z^2 = \tilde{v}^2 + G^2\tilde{u}^2 + K^2\tilde{w}^2 \qquad (2)$$

where G and K are the pitch and yaw factors defined by Jorgensen[10] and deduced from the calibration curves. Hence, equations for the effective cooling velocity can now be obtained for each of the six wire orientations. The effective cooling velocity is a function of the mean and fluctuating voltage. A Taylor series expansion can be carried out on Eq. (1) in terms of the effective cooling velocity. This expansion is truncated after the second-order terms with the assumption that higher-order terms are relatively small. This inclusion of second-order terms eliminates the necessity for assuming that the fluctuations are small with respect to the mean velocity. Solving simultaneously *any three adjacent equations* provides expressions for the instantaneous values of the three velocity components (u, v, and w in facility x, r and θ coordinates, respectively) in terms of the equivalent cooling velocities. It is then possible to obtain the three time-mean velocity components and the six different components of the Reynolds stress tensor in the manner described in Refs. 1 and 3.

Dvorak and Syred[6] used a DISA time correlator (55A06) to find the correlation coefficients between the velocity fluctuations in the three directions. One approach is to use the information obtained by all six orientations and to devise a mathematical procedure to calculate the covariances. These are calculated using the relationship

$$K_{Z_iZ_j} = \gamma_{Z_iZ_j}[\sigma^2_{Z_i}\sigma^2_{Z_j}]^{1/2} \qquad (3)$$

where $\gamma_{Z_iZ_j}$ is the correlation coefficient between the two cooling velocities Z_i and Z_j. By definition, the absolute value of the correlation coefficient $\gamma_{Z_iZ_j}$ is always less than 1.

Certain assumptions are made in order to calculate the covariances. However, King[8] observed that at times the calculated value of the correlation coefficient is greater than one at which instance he assigned previously fixed values to the correlation coefficients. It may be deduced that if two

wires are separated by an angle of 30 deg, the fluctuating signals from the wires at the two locations will be such that their contribution to the cooling of the wire will be related by the cosine of the angle between the wires. This assumption leads to the following three values of the correlation coefficients:

$$\gamma_{z_P z_Q} = \cos 30 \text{ deg} = 0.867$$

$$\gamma_{z_Q z_R} = \cos 30 \text{ deg} = 0.867 \tag{4}$$

The correlation coefficients may be related via[8]

$$\gamma_{z_P z_R} = \eta \gamma_{z_P z_Q} \gamma_{z_Q z_R} \tag{5}$$

where η is given a value of 0.8. Hence,

$$\gamma_{z_P z_R} = (0.8)(0.867)(0.867) = 0.6 \tag{6}$$

The three covariances are then obtained by substituting the corresponding values of the correlation coefficients into Eq. (3). King[8] used the above technique. The present study, however, uses Eqs. (4) and (6) during the entire data reduction. This simplification is justified a posteriori in Sec. V, where it is demonstrated that deduced results are relatively insensitive to correlative term inaccuracy.

III. Directional Sensitivity Analysis

The analysis is performed at any specific flowfield location by initially placing the probe in a free jet such that the coordinate system of the probe coincides with the coordinate system of the jet, as shown in Fig. 2a. Measurements are then taken by rotating the probe in the manner of the technique just described. To simulate the effect of the flow shifting its dominant flow direction, the probe is rotated by θ deg about its z axis, as shown Fig. 2b. This rotation causes a misalignment between the probe coordinate system and the facility coordinates. This discrepancy can be accounted for by use of the Eulerian matrices described in Sec. IV. In this configuration, the measured time-mean values and the normal and shear stresses are in a coordinate system oblique to the jet coordinate system. However, they can be transformed back to the facility coordinate system.[11] Notice that the correct directional sense of the rotation must be followed so that standard coordinate transformations may be used on the probe data so as to obtain facility coordinate data. Results shown later in Sec. V have been obtained in this manner.

To examine the directional sensitivity of the wire further, the probe was subsequently rotated about its new x axis, thereby forming a compound angle between the probe and the dominant flow velocity, as also shown in Fig. 1, see Fig. 2c. Again, the time-mean velocities and Reynolds stress tensor can be deduced in terms of the jet coordinate system by the method shown in Sec. IV and the results and their accuracy are discussed in Sec. V.

Specifically, the directional sensitivity of the technique is assessed at *five* flowfield situations for self-consistency using the following *five* configurations:

Case 1	$\theta = 0$ deg	$\theta = 0$ deg
Case 2	$\theta = -45$ deg	$\theta = 0$ deg
Case 3	$\theta = -45$ deg	$\theta = -45$ deg
Case 4	$\theta = -90$ deg	$\theta = 0$ deg
Case 5	$\theta = -90$ deg	$\theta = -90$ deg

The above *five* probe/flow configurations are used at each of *five* representative situations in a free axisymmetric nonswirling jet at $x/d = 0$ (laminar in potential core region), 3 and 10 (turbulent in shear layer region), and in a free axisymmetric swirling jet at a location in a region of strong shear just downstream of the exit from a variable-angle vane swirler with swirl vane angles of 45 and 70 deg representing moderate and strong swirl cases. In these swirling jet cases, the probe was located just downstream of the swirler exit, outside of any regions of recirculation. This part of the flow was chosen as it is in an area of rapid acceleration and is unlikely to contain any instantaneous flow reversals that might cause erroneous readings. This is because hot-wire sensors have the fundamental disadvantage of being unable to distinguish between forward and reverse flow. This causes a serious problem with hot wires in instantaneous flow reversal situations, which occur predominantly on the edges of the recirculation zones. It is expected that any measurements taken in these regions will be subject to some degree of error. Specifically, the following *five* situations are used:

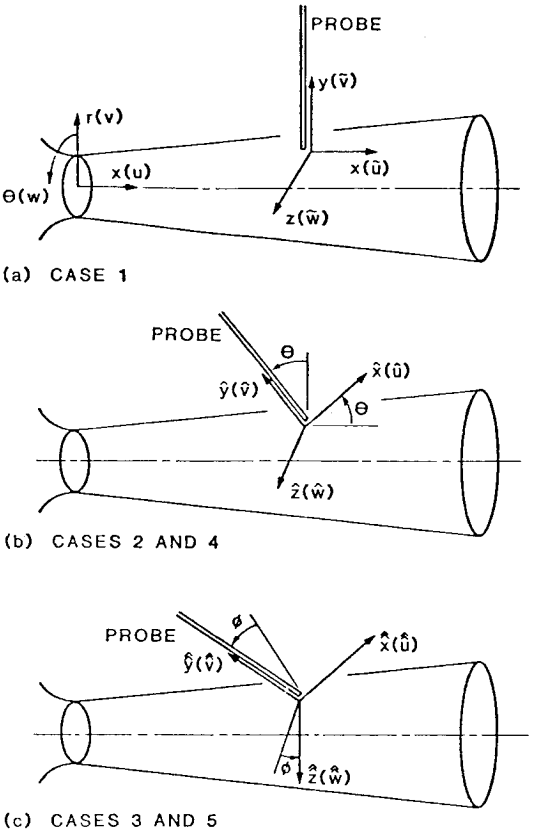

Fig. 2 Configurations used in the directional sensitivity study.

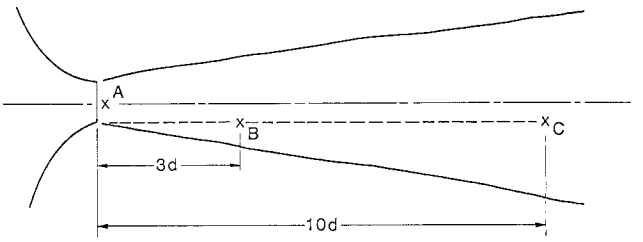

Fig. 3 Free nonswirling jet measurement locations for situations A-C.

Situation A	$x/d = 0$	nonswirling laminar region
Situation B	$x/d = 3$	nonswirling turbulent region
Situation C	$x/d = 10$	nonswirling turbulent region
Situation D	$x/d = 0$	swirling turbulent region with swirl vane angle 45 deg
Situation E	$x/d = 0$	swirling turbulent region with swirl vane angle 70 deg

These locations are illustrated in Figs. 3 and 4. It will be seen later that the sensitivity analysis assures users that

knowledge of local configuration of probe vs flow direction is not required *a priori* and useful results are forthcoming and relatively insensitive to specific configurations.

IV. Coordinate Transformation

To investigate the shifting of the dominant flow direction, the probe holder vs local time-mean flow vector configuration is varied through *five* different cases of interest. To relate probe coordinate data back to the facility coordinate system, use is made of Eulerian rotational matrices. These make it possible to relate all time-mean velocities and the full Reynolds stress tensor back to the facility coordinate system after any axis rotation. The required matrix transformations are given in Ref. 2.

V. Results

Uncertainty Analysis

The uncertainty analysis includes a determination of the sensitivity of the six-orientation hot-wire data reduction to various input parameters having major effects on the response equations. Pitch and yaw factors (G and K) are used in the response equations described in Sec. II in order to account for the directional sensitivity of the single hot-wire probe. Both the pitch and yaw factors are functions of the hot-wire mean effective voltage, but the yaw factor is far more sensitive. A 1% increase in the hot-wire voltage reduces the pitch factor by 1.3% and the yaw factor by 56%.[1-3] For the present study, the values of these factors are chosen at an average hot-wire voltage experienced in the flowfield. This was appropriate since the output quantities (u, u'_{rms}, $\overline{u'v'}$, etc) are only weakly dependent on the value of K. This can be seen in the data of Table 1, which summarizes an analysis performed on the data reduction program at a representative position in the flowfield.

Table 1 demonstrates the percent change in the output quantities for a 1% change in most of the important input quantities. For the data presented in this table, only quantities calculated from the probe orientation combination 5, 6, and 1 are used, for simplicity. The situation is that of a moderately swirling confined flowfield from a swirl generator with vane angle of 38 deg. In this swirling flow, orientation 6 was the minimum of the six mean effective cooling velocities. King[8] has argued that the probe orientation combination approximately centered around the minimum effective cooling velocity produces more accurate estimates of calculated turbulence quantities than do the other orientation combinations. However, all previously reported data have been obtained by averaging all the six possible combinations.

It is not unusual in hot-wire anemometry for the mean velocity components and turbulence quantities to be quite sensitive to changes in the mean hot-wire voltage. For interpretive purposes, the mean hot-wire voltage variations can be thought of as being either errors in measuring the mean voltage or shifts in the individual wire calibrations due to contamination or strain "aging" of the wire. The data of Table 1 demonstrate that the most serious inaccuracies in the measurement and data reduction technique will be in the estimates of turbulent shear stresses, the most inaccurate output term being $\overline{u'w'}$.

As already discussed in Sec. II, an *ad hoc* assumption is made regarding the numerical values of the correlation coefficients used in the deduction of time-mean and turbulence quantities. The results of the uncertainty analysis (Table 1) show the time-mean and turbulence quantities to be relatively insensitive to variations in the correlation coefficients. Therefore, the major *ad hoc* assumption made in the technique does not seem to have a great effect on the output quantities compared to the effect of other input quantities.

Laminar Jet

The directional sensitivity of the technique was assessed at the five locations A-E (see Figs. 3 and 4) corresponding to five

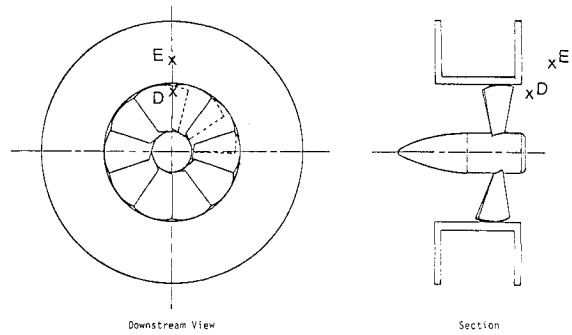

Fig. 4 Free swirling jet measurement locations for situations D and E.

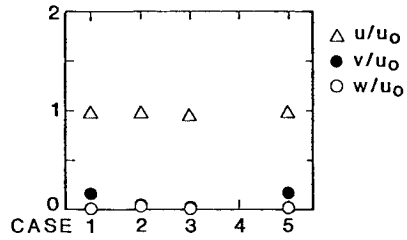

Fig. 5 Measurements for situation A with different probe configuration cases.

Table 1 Effect of input parameters on turbulence quantities in a confined swirling flow with swirl vane angle of 38 deg at a representative flowfield position ($x/D = 1$, $r/D = 0.25$)

Parameter	Change in parameter, %	Change in time-mean and turbulence quantities, %								
		$\bar{u}$	$\bar{v}$	$\bar{w}$	u'_{rms}	v'_{rms}	w'_{rms}	$\overline{u'v'}$	$\overline{u'w'}$	$\overline{v'w'}$
$\bar{E}_1$	+1	+16.10	+0.66	+4.98	+15.75	−2.06	+2.75	+6.0	+51.43	+11.94
$\bar{E}_5$	+1	+2.19	−2.21	+11.49	−6.50	+2.42	+12.88	+4.0	+14.29	+7.46
$\bar{E}_6$	+1	−10.59	−0.36	−8.50	−1.88	+7.07	−9.54	−6.0	−54.29	−11.94
$\bar{E}'_{1_{rms}}$	+1	+0.27	−0.06	+0.14	+1.63	+0.13	+0.39	+2.0	+2.86	+1.49
$\bar{E}'_{5_{rms}}$	+1	+0.05	0.0	+0.14	0.0	−0.13	+1.57	0.0	0.0	+1.49
$\bar{E}'_{6_{rms}}$	+1	−0.16	+0.18	−0.14	−0.63	+1.03	−1.08	−2.0	−5.71	0.0
G	+1	−1.02	0.0	−1.01	−1.0	0.0	−0.98	−2.0	−2.86	−1.49
K	+1	+0.01	−0.04	+0.01	+0.01	0.0	+0.01	0.0	0.0	0.0
$\gamma_{Z_PZ_Q}$	+1	+0.05	0.0	+0.14	−0.13	−0.13	−1.77	0.0	−2.86	+1.49
$\gamma_{Z_QZ_R}$	+1	+0.21	+0.01	+0.05	−1.63	+0.13	−0.79	0.0	−5.71	+1.49
$\gamma_{Z_PZ_R}$	+1	−0.16	+0.18	−0.08	+0.13	+0.0	+0.69	−2.0	+2.86	0.0

different flow situations. Table 2 gives a summary of the measurements by presenting the ensemble average $\bar{x}$ of the deduced results from each of the six possible combinations of three adjacent wire orientations and the coefficient of variation $\sigma/\bar{x}$, where σ is the standard deviation of the six values about the mean. The first configuration is situation A with measurements in the laminar potential core region, at $x/d=0$ and $r/d=0$. The first data set in Table 2 gives the results with the probe coordinates aligned with facility coordinates, as case 1 of Fig. 2 illustrates. This is referred to as situation A/case 1 with analogous statements used for other configurations as well. The time-mean velocities, nondimensionalized with the jet exit velocity deduced from an independent measurement, are shown. In this one-dimensional flowfield, the axial velocity is expected to be unity with the other two components of the velocity vector to be equal to zero. Results using each of the six possible combinations of three adjacent wire orientations are simply averaged and the mean $\bar{x}$ of the values is given. The ratio of standard deviation to the mean $\sigma/\bar{x}$, called the coefficient of variation, is also presented to show the amount of scatter in the readings. As can be seen, the scatter for the axial and swirl velocities is very low for each combination. The radial velocity scatter tends to be larger, but is less significant because of the low mean value of radial velocity. The mean of these quantities brings the data to well within acceptable limits.

Results of the probe being rotated by 45 deg about the z axis (as in case 2 with $\theta=-45$ deg) are also shown in Table 2. This

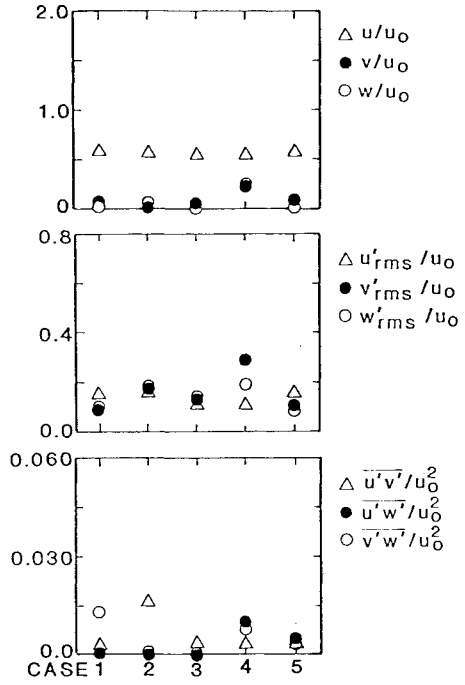

Fig. 6 Measurements for situation B with different probe configuration cases.

Table 2 Ensemble average $\bar{x}$ and coefficient of variation $\sigma/\bar{x}$ measurements

Situation/ case		u/u_0	v/u_0	w/u_0	u'_{rms}/u_0	v'_{rms}/u_0	w'_{rms}/u_0	$\overline{u'v'}/u_0^2$	$\overline{u'w'}/u_0^2$	$\overline{v'w'}/u_0^2$
A/1	$\bar{x}$	0.970	0.147	0.013						
	$\sigma/\bar{x}$	0.006	0.503	0.353						
A/2	$\bar{x}$	0.983	0.021	0.033						
	$\sigma/\bar{x}$	0.006	0.553	0.353						
A/3	$\bar{x}$	0.958	−0.039	0.001						
	$\sigma/\bar{x}$	0.009	0.805	38.986						
A/5	$\bar{x}$	0.969	0.147	0.013						
	$\sigma/\bar{x}$	0.006	0.503	0.317						
B/1	$\bar{x}$	0.593	0.189	0.030	0.149	0.084	0.105	0.0031	0.0012	0.0129
	$\sigma/\bar{x}$	0.022	0.212	0.537	0.98	0.718	0.330	1.1910	0.9350	0.7130
B/2	$\bar{x}$	0.546	0.010	0.092	0.159	0.161	0.170	0.0163	−0.0014	0.0014
	$\sigma/\bar{x}$	0.037	4.600	0.493	0.177	0.170	0.369	2.2371	1.7875	1.7875
B/3	$\bar{x}$	0.556	0.046	−0.017	0.117	0.123	0.128	0.0031	−0.0088	−0.0024
	$\sigma/\bar{x}$	0.018	0.429	0.669	0.159	0.188	0.183	2.9016	2.7612	6.0300
B/4	$\bar{x}$	0.549	0.212	0.238	0.111	0.285	0.184	0.0032	0.0109	0.0083
	$\sigma/\bar{x}$	0.083	0.589	0.546	0.221	0.259	0.446	0	1.4700	1.2864
B/5	$\bar{x}$	0.583	0.205	0.035	0.159	0.116	0.082	0.0035	0.0054	0.0035
	$\sigma/\bar{x}$	0.076	0.357	0.573	0.053	0.320	0.465	0.9143	0.6490	0.4571
C/1	$\bar{x}$	0.456	0.144	0.023	0.130	0.062	0.083	0.0038	0.0011	0.0037
	$\sigma/\bar{x}$	0.032	0.182	0.396	0.068	0.112	0.353	0.6468	0	0.5833
C/2	$\bar{x}$	0.445	0.066	0.019	0.119	0.119	0.121	0.0160	0.0013	0.0012
	$\sigma/\bar{x}$	0.020	0.561	0.862	0.111	0.111	0.169	0.3861	0.6421	1.0000
C/3	$\bar{x}$	0.446	0.048	−0.060	0.098	0.094	0.102	0.0049	0.0044	0.0063
	$\sigma/\bar{x}$	0.035	0.713	0.707	0.154	0.153	0.145	2.1632	3.1641	1.3516
C/4	$\bar{x}$	0.343	0.228	0.176	0.098	0.252	0.237	0.0149	0.0107	0.0507
	$\sigma/\bar{x}$	0.107	0.602	0.368	0.113	0.210	0.223	0.7584	0.5047	0.5355
C/5	$\bar{x}$	0.446	0.029	0.147	0.147	0.089	0.047	0.0036	0.0038	0.0044
	$\sigma/\bar{x}$	0.044	0.717	0.249	0.046	0.473	0.214	0.2608	0.4676	0.6735
D/1	$\bar{x}$	1.739	0.585	1.613	0.134	0.149	0.123	0.0064	0.0057	0.0082
	$\sigma/\bar{x}$	0.029	0.038	0.034	0.213	0.225	0.158	0.1983	0.6131	0.3321
D/4	$\bar{x}$	1.641	0.833	1.525	0.121	0.140	0.133	0.0037	0.0032	0.0044
	$\sigma/\bar{x}$	0.089	0.107	0.051	0.120	0.234	0.226	0.3690	0.8348	0.7578
D/5	$\bar{x}$	1.802	0.409	1.447	0.142	0.158	0.186	0.0068	0.0007	0.0142
	$\sigma/\bar{x}$	0.036	0.175	0.050	0.026	0.224	0.492	0.7682	0.3571	0.4571
E/1	$\bar{x}$	0.624	0.458	0.403	0.437	0.219	0.422	0.0424	0.0295	0.0362
	$\sigma/\bar{x}$	0.130	0.263	0.110	0.256	0.451	0.315	0.2846	1.0975	0.3903
E/4	$\bar{x}$	0.521	0.394	0.382	0.373	0.561	0.704	0.0271	0.0440	0.0288
	$\sigma/\bar{x}$	0.302	0.414	0.476	0.007	0.410	0.154	0.5251	0.6197	0.0582
E/5	$\bar{x}$	0.599	0.220	0.508	0.534	0.416	0.300	0.0245	0.0163	0.0425
	$\sigma/\bar{x}$	0.225	0.331	0.318	0.202	0.349	0.231	0.4773	0.5958	0.6824

is situation A/case 2. The probe coordinate system is now different from the jet coordinate system, but the measured velocities can be related to the facility coordinates by use of the rotational matrices given in Sec. IV. All values in the tables are presented in terms of the facility coordinate system. The results show that this misalignment of the probe with the dominant flow direction still gives excellent values of velocities in the laboratory coordinate system with the use of any of the six possible wire combinations. Consequently, averaging of the data also gives good results.

Rotation about the z axis by -90 deg to obtain case 4 results in no data being generated by the technique. This is because in a steady one-dimensional flowfield all the instantaneous cooling velocities acting on the hot wire are equal for all six orientations. As the data analysis requires that their cooling velocities be subtracted from each other (see Ref. 3), all the output terms are deduced as zero.

To further investigate the shifting of the dominant flow direction, the probe was rotated twice (-45 deg about its z axis, followed by -45 deg about its new x axis) so as to conform to case 3. The results of these axis rotations can be seen in Table 2. Again, the laboratory coordinate deduced values are presented and deviations from expected values are relatively low, although not quite as good as in the previous case. The advantages of averaging can be seen, where the under- and/or overestimation of the velocities for the individual positions are smoothed after averaging.

Rotations of $\theta = -90$ deg and $\phi = -90$ deg were also carried out at the same flow location, thus obtaining case 5. Good axial and tangential velocity values can also be seen in the table but with a decrease in the accuracy of the radial velocity. Figure 5 gives a summary of the ensemble-averaged data (obtained from the six possible combinations of three adjacent wire orientations being used for data reduction). It reveals very clearly that the measurements in facility coordinates are quite insensitive to probe holder vs facility configuration.

Turbulent Nonswirling Jet

Similar probe configurations (cases 1-5) have been performed on the shear layer of a free nonswirling axisymmetric jet at two axial locations, $x/d = 3$ and 10, referred to as situations B and C. Results are included in Table 2 with ensemble-averaged data assembled in Figs. 6 and 7 for visual impact. The style of these figures is the same as Fig. 5 and again the changes to deduced quantities are seen for the different cases of probe configuration vs main flow direction. In general, the scatter is within tolerable limits. Table 2 included further details, which are discussed below.

At these points in the flow, the axial velocity dominates with a small contribution from the radial velocity. In axisymmetric jets, it is well known that the axial directional turbulence intensity is larger than its other two components.[11,12] The only significant shear stress in this flowfield is the rx shear. Results in Table 2 obtained with case 1 probe configuration in situations B and C confirm this. Incidently, all of the data presented in this paper are a consequence of a typical set of readings obtained from the hot-wire technique. If a large amount of scatter is found in the deduced results at a particular location, the problem is further investigated and/or remeasured before being accepted as valid. Data reported elsewhere[3,4] has been thoroughly analyzed and checked for repeatability.

The case 1 data at locations B and C are used as a standard for nonswirling flowfield values, so as to be able to compare the results obtained from other probe configuration cases. However, the radial time-mean velocity appears to be very large for this particular flowfield and could possibly be in error. The coefficient of variation $\sigma/\bar{x}$ is seen to be acceptable for most of the flow properties except for the shear stresses. These large variations are caused by the shear stresses being two orders of magnitudes lower than the time-mean velocities. Sometimes the data reduction will not resolve a particular parameter. This is usually the consequence of subtracting two almost equal effective cooling velocities, as described earlier. If a large proportion of the data is not resolved from the different combinations of cooling velocities used, the parameter deduced is taken to be zero.

Results for probe configurations of cases 2 and 4 for locations B and C may also be analyzed. It can be seen that the case 4 results give poor estimates of the time-mean radial and swirl velocities and underestimates of the axial components of the velocity vector. This is expected because the time-mean velocity vector is almost parallel to the hot-wire support axis and rotating the probe through its six orientations has little effect on the sensed data. This also decreases values of the axial turbulence intensity, but significantly increases the other two normal stress components. Shear stress values for cases 2 and 4 are found to be very poor with large coefficients of variation. Also, many of the turbulence quantities are not resolved. It would appear from these results that the six-orientation hot-wire technique is a poor tool to use if the flow is dominantly in the direction of the probe support, for the reasons just described. If this occurs, simply reconfiguring the probe holder vs flow direction can overcome the problem.

Cases 3 and 5 at locations B and C may be observed and compared with the previous cases 2 and 4 at these same locations. Now the time-mean velocity components are seen to be in excellent agreement with the values determined from the standard configuration of case 1. The axial normal stress tends to be underestimated at $x/d = 3$ and overestimated at $x/d = 10$, relative to the case 1 calculations. The radial turbulence intensity is consistently overestimated for both compound configurations and both axial locations. This could infer a failing of the hot-wire technique. The tangential turbulence intensity mesurements are found to provide acceptable results. The dominant shear stress (the rx component) in this flow is found to be measured very well in the configurations of cases 3 and 5, relative to case 1 values. The coefficient of variation is not too large considering the magnitude of the numbers involved. The final components of the Reynolds stress tensor, although appearing to be measurable, exhibit a great deal of scatter, perhaps indicating that these values are close to zero.

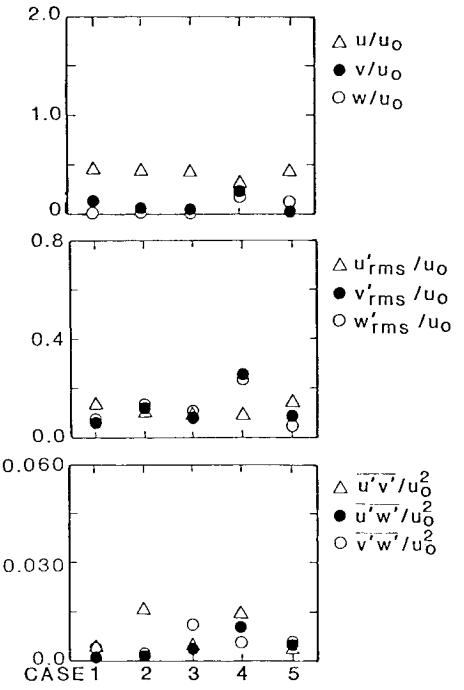

Fig. 7 Measurements for situation C with different probe configuration cases.

Turbulent Swirling Jet

Two free swirling jets were considered for further assessment of the hot-wire technique. The airflow exiting from an axisymmetric nozzle of a wind tunnel passes through a vane swirler with 10 adjustable flat blades. The test facility and time-mean performance of the swirler are described at length in Ref. 13. For the present study, the subsequent large chamber confinement was removed and the free jet flow alone was studied, with swirl vane angles of 45 and 70 deg being used. Figure 3 gives the specific measurement locations D and E used for measuring the 45 and 70 deg swirl situations, respectively. These locations are in the high-shear region of the flow close to the swirler exit. They were chosen since it was expected that all six components of the stress tensor would be significant, thereby providing a good test of the technique for their measurement. The hot wire was also placed well away from the edge of the recirculation zone, so as to avoid any instantaneous flow reversal on the wire. Measurements conforming to cases 1, 4, and 5 have been made for both of the swirl strengths. The relevant data also appear in Table 2 with Figs. 8 and 9 summarizing the ensemble-averaged data over the cases investigated. The increase in the turbulence properties of the flow is clearly evident as the swirl strength increases, even though the D and E locations are not coincident.

Rotation about the z axis by -90 deg to case 4 probe configuration causes a deterioration in the accuracy of the results obtained from the technique, as inspection of the case 4 results for situations D and E reveals. The axial and swirl time-mean velocities are still fairly accurate for both flows, but the radial velocity has suffered a large increase relative to its measurment with case 1. The normal stresses deduced after the rotation appear to be reasonable. The shear stresses show a reduction in accuracy, with all three components either over- or underpredicting the case 1 values. It is again felt that these poor results are because of the technique's inability to measure flow properties accurately when the dominant flow direction is in the direction of the probe holder. That is, when a large velocity is approximately normal to the wire in each of the six measuring orientations, insensitivity results, as already discussed earlier.

The results of the compound angle of case 5 are presented in Table 2 for the 45 and 70 deg swirl cases of situations D and E, respectively. The axial time-mean velocity is seen to be good when compared to the standard case, but the other two components show a reduction in accuracy in these highly turbulent flowfields. The inaccuracy of the radial velocity was discussed earlier. The three components of the turbulence intensity appear to be fairly good with reasonable values deduced compared to the standard case 1 values. Again, however, the radial and tangential component are less than desirable for the strongly swirling flowfield. The shear stresses for the 45 deg swirl situation D are considered good except for the $\overline{u'w'}$ term. This component is subject to great inaccuracies for only slight errors in this input data, as described above.

Assessment of the Technique

General results of the present and previous studies are now assessed in connection with the applicability, accuracy, and directional sensitivity of the six-orientation, single normal hot-wire technique.

Previously, in his measurements of strongly swirling vortex flows, King[8] compared his time-mean velocity and *normal* stress measurements with corresponding measurements obtained using a laser Doppler velocimeter (LDV). He found excellent agreement indicating the validity of the method. He was not able to compare *shear* stress measurements in his *swirl* flow, however, because he was unable to use his LDV for this purpose. In fact, despite the existence of advanced multicolor LDV systems and their use for shear stress measurement, no one has yet reported them in highly swirling flow situations: certainly not over a range of swirl strengths as reported in Ref. 5.

The present authors have already compared their six-orientation measurements with previously available data whenever possible, including nonswirling[14,15] and swirling[16,17] data. Results are useful in recent prediction studies for confined swirling flows.[18-20]

For the present study, Figs. 5-9 summarize measured values for the five situations A-E, respecitively. Each figure presents facility coordinate time-mean velocity, normal and shear stress values obtained with each of the five probe holder vs

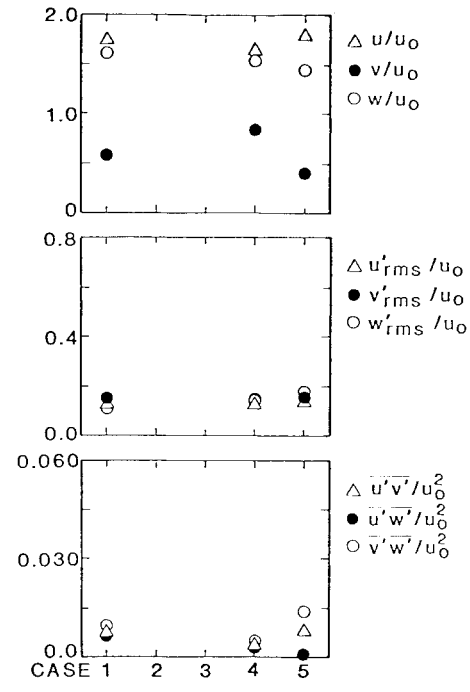

Fig. 8 Measurements for situation D with different probe configuration cases.

Table 3 Comparison of averaged results from six possible wire combinations with "optimal" combination

Situation		u/u_0	v/u_0	w/u_0	u'_{rms}/u_0	v'_{rms}/u_0	w'_{rms}/u_0	$\overline{u'v'}/u_0^2$	$\overline{u'w'}/u_0^2$	$\overline{v'w'}/u_0^2$
					Measured					
A	345	0.968	NR[a]	0.013						
	$\bar{x}$	0.970	0.147	0.013						
B	345	0.587	0.110	0.019	0.125	0.209	0.126	0.0001	0.0000	NR
	$\bar{x}$	0.593	0.189	0.030	0.157	0.084	0.105	0.0031	0.0012	0.0129
C	345	NR								
	$\bar{x}$	0.456	0.144	0.023	0.130	0.062	0.083	0.0037	0.0011	0.0036
D	561	1.702	0.665	1.609	0.138	0.091	0.108	0.0043	0.0045	0.0066
	$\bar{x}$	1.739	0.585	1.613	0.134	0.149	0.123	0.0064	0.0057	0.0082
E	561	0.628	0.323	0.478	0.463	0.135	0.525	0.0384	0.0411	NR
	$\bar{x}$	0.624	0.458	0.403	0.437	0.219	0.422	0.0424	0.0295	0.0362

[a]Not resolved.

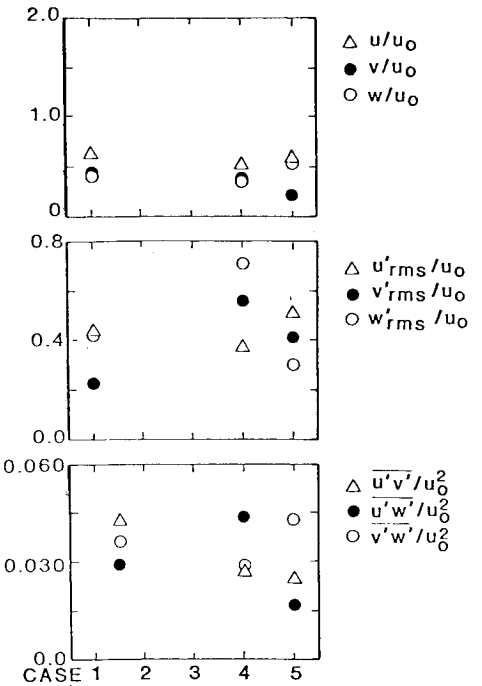

Fig. 9 Measurements for situation E with different probe configuration cases.

facility configuration possibilities of cases 1-5. A remarkable observation is that, in general, the configuration is of little importance—the results appearing quite constant across the five cases.

On the other hand, production run results[1-5] have used the case 1 configuration exclusively. In those results, generally, an ensemble average of the deduced results from each of the six possible combinations of three adjacent wire orientations has been used. This was because of a lack of local flow directional knowledge—if this knowledge is available, it is expected[8] that the combination with minimum cooling velocity in the central of the three wire orientations used will produce more accurate estimates of deduced flow quantities. From results of the present study for situation A-E, Table 3 presents the "optimal" values and the ensemble-averaged values. Surprisingly, the values are quite comparable. In any case, the appropriate choice of wire orientation for minimum cooling velocity is not known *a priori*. The values given in the table could be determined only after the measurement. However, for turbulence quantities and in the 45 and 70 deg situations, more confidence may be placed in the average of all possible wire combinations. This smoothing has been used exclusively in recent studies.[1-5]

VI. Conclusions

The accuracy and directional sensitivity of the six-orientation hot-wire technique has been performed in axisymmetric and swirling free jets. Variation of input parameters and their effect on the output data has shown that the least accurate output quantities are the shear stresses, in particular, the $x\theta$ component. The directional sensitivity analysis has shown that the technique adequately measures the properties of a flowfield independent of the dominant flow direction except when the flow is predominately in the direction of the probe holder, with the six orientations of the probe then creating insignificant changes in hot-wire response. Results also show that the component of time-mean velocity in the probe holder direction is inadequately deduced. Only reconfigurating of the probe can overcome this problem *a posteriori*.

Acknowledgments

The authors wish to extend there gratitude to NASA Lewis Research Center and the Air Force Wright Aeronautical Laboratories for their support under Grant NAG 3-74, technical monitor Dr. J. D. Holdeman. Thanks are also given to Lawrence H. Ong for assistance with the experiments.

References

[1]Janjua, S. I., "Turbulence Measurements in a Complex Flowfield Using a Six-Orientation Hot-Wire Probe Technique," M. S. Thesis, Oklahoma State University, Stillwater, Dec. 1981.

[2]Jackson, T. W., "Turbulence Characteristics of Swirling Flowfields," Ph.D. Thesis, Oklahoma State University, Stillwater, Dec. 1983.

[3]Janjua, S. I., McLaughlin, D. K., Jackson, T. W., and Lilley, D. G., "Turbulence Measurements in a Confined Jet Using a Six-Orientation Hot-Wire Probe Technique," AIAA Paper 82-1262, June 1982.

[4]Janjua, S. I., McLaughlin, D. K., Jackson, T. W., and Lilley, D. G., "Turbulence Measurements in Confined Jets Using a Rotating Single-Wire Probe Technique," *AIAA Journal*, Vol. 21 Dec. 1983, pp. 1609-1610.

[5]Jackson, T. W. and Lilley, D. G., "Single-Wire Swirl Flow Turbulence Measurements," AIAA Paper 83-1202, June 1983.

[6]Dvorak, K. and Syred, N., "The Statistical Analysis of Hot Wire Anemometer Signals in Complex Flowfields," Paper presented at DISA Conference, University of Leicester, England, 1972.

[7]Syred, N., Beer, J. M., and Chigier, N. A., "Turbulence Measurements in Swirling Recirculating Flows," *Proceedings of Salford Symposium on Internal Flows*, Institution of Mechanical Engineers, London, 1971, pp. B27-B36.

[8]King, C. F., "Some Studies of Vortex Devices-Vortex Amplifier Performance Behavior," Ph.D. Thesis, University College of Wales, Cardiff, 1978.

[9]Arterberry, S. H. "An Improved Method to Flowfield Determination in Three-Dimensional Flows of Low Intensity and Moderate Skewness," M.S. Thesis, University of Washington, Seattle, 1982.

[10]Jorgensen, F. E., "Directional Sensitivity of Wire and Fiber Film Probes," DISA Information No. 11, May 1971, pp. 31-37.

[11]Yuan, S. W., *Foundations of Fluid Mechanics,* Prentice-Hall, Englewood Cliffs, NJ, 1967.

[12]Corrsin, S. and Uberoi, M.S., "Spectrums and Diffusion in a Round Turbulent Jet," NACA Rept. 1040, 1949.

[13]Sander, G. F. and Lilley, D. G., "The Performance of an Annular Vane Swirler," AIAA Paper 83-1326, June 1983.

[14]Chaturvedi, M. C., "Characteristics of Axisymmetric Expansions," *Proceedings, Journal of the Hydraulics Division, ASCE,* Vol. 89, No. HY3, 1963, pp. 61-92.

[15]McKillop, B. E., "Turbulence Measurements in a Complex Flowfield Using a Crossed Hot-Wire," M.S. Thesis, Oklahoma State University, Stillwater, July 1983.

[16]Janjua, S. I. and McLaughlin, D. K., "Turbulence Measurements in a Swirling Confined Jet Flowfield Using a Triple Hot-Wire Probe," Rept. DT-8178-02 from Dynamics Technology to NASA Lewis Research Center, Nov. 1982.

[17]Yoon, H. K. and Lilley, D. G., "Five-Hole Pitot Probe Time-Mean Velocity Measurements in Confined Swirling Flows," AIAA Paper 83-0315, Jan. 1983 (also, "Further Time-Mean Measurements in Confined Swirling Flows," *AIAA Journal*, Vol. 22, April 1984, pp. 514-515).

[18]Abujelala, M. T. and Lilley, D. G., "Confined Swirling Flow Predictions," AIAA Paper 83-0316, Jan. 1983.

[19]Abujelala, M. T. and Lilley, D. G., "Limitations and Empirical Extensions of the k-ϵ Model as Applied to Turbulent Swirling Flows," AIAA Paper 84-0441, Jan. 1984.

[20]Abujelala, M. T., Jackson, T. W., and Lilley, D. G., "Swirl Flow Turbulence Modeling," AIAA Paper 84-1376, June 1984.